Research Square

Preprints are preliminary reports that have not undergone peer review.
They should not be considered conclusive, used to inform clinical practice,
or referenced by the media as validated information.

RNA-seq Identifies FOS as a Potential Therapeutic Target Activating Neural Stem Cells via miR-21/SOX2 Pathway in Hypertensive Intracerebral Hemorrhage

Wei Dai
Minhang Hospital, Fudan University
Jiarui Du
Minhang Hospital, Fudan University
Fulin Xu
Minhang Hospital, Fudan University
Zuopeng Su
suzuopeng@163.com

Minhang Hospital, Fudan University

Article

Keywords: Hypertensive intracerebral hemorrhage, RNA-seq, FOS, Neural stem cells, miR-21/SOX2 pathway

Posted Date: July 7th, 2026

DOI: https://doi.org/10.21203/rs.3.rs-9806137/v1

License: This work is licensed under a Creative Commons Attribution 4.0 International License.
Read Full License

Additional Declarations: No competing interests reported.

Abstract

Objective

Intracerebral hemorrhage (ICH) is a severely devastating neurological disorder. At present, there is no specific effective therapy for ICH, and its pathophysiological mechanism remains incompletely elucidated. Herein, we attempted to identify blood mRNA biomarkers, potential therapeutic targets and pathways associated with ICH via RNA sequencing.

Results

Biological analysis of RNA-seq data screened numerous differentially expressed genes involved in various biological processes including inflammation, immunity and regeneration, which were systematically summarized in this study. Through bioinformatic analysis and experimental validation, we found that the expression level of *FOS* gene was upregulated after ICH, with the potential to participate in the proliferation and differentiation of neural stem cells and promote neural recovery. Our research further indicated that Fos may be involved in the regulation of biological behaviors of neural stem cells via the miR-21/SOX2 signaling pathway, although its exact mode of action requires further investigation.

Conclusion

Collectively, RNA-seq delineated the precise transcriptional alterations in peripheral blood between patients with hypertensive intracerebral hemorrhage and hypertensive control subjects. These findings establish a potential therapeutic target centered on the *FOS* gene, which is aimed at activating neural stem cells following intracerebral hemorrhage.

Introduction

Intracerebral hemorrhage (ICH) is a devastating disease and a subtype of stroke. Although it accounts for only 27.9% of all stroke cases, ICH typically leads to severe outcomes such as death and lifelong disability. Globally, stroke was the second leading cause of combined death and disability and the third leading cause of death in 2019.[1] The incidence of ICH is higher in low- and middle-income countries than in high-income countries.[2] In recent years, with increased attention and control of blood pressure, the incidence of ICH has declined compared with previous years; nevertheless, ICH still imposes a substantial medical and economic burden on developing countries.[3]

Pathophysiologically, during the initial injury phase, rupture of small intracerebral arteries results in hematoma formation, which in turn causes mechanical damage via mass effect on the brain parenchyma and disrupts brain tissue architecture.[4] As the disease progresses, secondary brain injury triggers microglial activation and the release of inflammatory and cytotoxic mediators, leading to blood-

brain barrier disruption, vasogenic edema, and neuronal cell death. [5–8] However, according to current guidelines, most patients with ICH do not undergo hematoma evacuation surgery due to the lack of definitive clinical benefit, as well as the potential for more severe complications and poorer prognosis.[9] Therefore, an increasing number of studies have focused on the roles of metabolites released during secondary brain injury in inflammation, edema, and blood-brain barrier damage (also referred to as SBI), [10] aiming to intervene in these processes to alleviate neurological deficits and improve quality of life after ICH.

In the present study, peripheral blood samples were collected from patients with hypertensive intracerebral hemorrhage and hypertensive control subjects, followed by bulk RNA sequencing. Subsequent bioinformatic analyses were performed to identify differentially expressed genes, and further investigations were conducted focusing on the FOS gene, confirming its potential as a therapeutic target for neurological recovery following hypertensive intracerebral hemorrhage.

Materials and Methods

Patients and Samples

We enrolled patients diagnosed with hypertensive intracerebral hemorrhage (HICH) and hypertensive individuals undergoing routine physical examination at Minhang Hospital, Fudan University, between September 2025 and January 2026. Peripheral venous blood samples were collected from all subjects. For HICH patients, blood samples were obtained within 24 hours after ictus.

Inclusion criteria for HICH patients:

1. Admission blood pressure > 140/90 mmHg with a prior diagnosis of hypertension and poor blood pressure control;

2. Age between 18 and 85 years;

3. Radiologically confirmed hypertensive intracerebral hemorrhage.

Exclusion criteria for HICH patients:

1. Severe primary diseases involving cardiac, hepatic, renal, or hematopoietic dysfunction;

2. Psychiatric disorders;

3. Intracerebral hemorrhage caused by vascular malformation, trauma, brain tumor, or other etiologies.

Hypertensive control subjects were matched with the HICH group for age and sex, presented with poorly controlled blood pressure (> 140/90 mmHg) on physical examination, and had normal general examination results without obvious positive signs.

This study was approved by the Ethics Committees of Shanghai Jiao Tong University and Minhang Hospital, Fudan University, and conducted in accordance with the principles of the Declaration of Helsinki. Written informed consent was obtained from each patient or their legal guardian prior to blood sample collection and subsequent experiments.

Isolation and Cryopreservation of Human Peripheral Blood Mononuclear Cells (PBMCs)

Peripheral venous blood was collected from the HICH group (within 24 hours after ictus) and the hypertensive control group. Blood samples were stored in anticoagulant-containing tubes at room temperature and processed within 4–8 hours to preserve cell viability.

PBMCs were isolated by density gradient centrifugation using Ficoll lymphocyte separation medium (density 1.077 ± 0.001 g/mL, pre-equilibrated to 18–20°C). Briefly, diluted or fresh whole blood was gently layered onto the separation medium at a 1:1 volume ratio, followed by centrifugation at 250×g (≈ 1200 rpm) for 20 minutes at room temperature with the brake disabled. The milky-white PBMC layer was carefully aspirated in a biological safety cabinet, washed twice by centrifugation at 250×g for 7 minutes in sterile phosphate-buffered saline (PBS, pH 7.2–7.4), and resuspended in complete RPMI-1640 medium supplemented with 10% heat-inactivated fetal bovine serum and 1% penicillin-streptomycin. Cell viability was verified by trypan blue exclusion to be ≥ 90%.

For cryopreservation, viable PBMCs were resuspended in freshly prepared freezing medium (90% heat-inactivated fetal bovine serum + 10% dimethyl sulfoxide) or a commercial serum-free freezing medium designed for PBMCs, transferred into cryovials, and gradually frozen at a rate of 1°C/min using a programmed freezing container. Samples were then stored long-term in a − 80°C ultra-low temperature freezer or in liquid nitrogen.

All materials and reagents were sterile and endotoxin-free. All procedures were performed under aseptic conditions to avoid microbial contamination.

RNA-seq

Subsequent bulk RNA-seq procedures were performed by TIANGEN Biotech Co., Ltd. (Beijing). RNA concentration and purity were assessed using a NanoDrop 2000 Spectrophotometer (Thermo Fisher Scientific), and RNA integrity was evaluated using an Agilent 2100 Bioanalyzer with the 2100 RNA Nano 6000 Assay Kit (Agilent Technologies).

Using total RNA that passed quality control as starting material, the TIANSeq mRNA Capture Kit (TIANGEN Biotech) was employed to enrich poly(A)-tailed RNA from eukaryotic total RNA. The enriched mRNA was then used as input for library construction with the TIANSeq Fast RNA Library Preparation Kit (Illumina platform) (TIANGEN Biotech). The library was constructed through a series of steps including RNA fragmentation, first- and second-strand cDNA synthesis, end repair, 3'-end adenylation, adapter ligation, and PCR enrichment.

After library construction, initial quantification was performed using a Qubit 2.0 Fluorometer, and libraries were diluted to 1 ng/μL. Insert size was then verified using the Agilent 2100 Bioanalyzer. Once insert size matched the expected range, the effective library concentration was accurately quantified by qPCR (effective concentration > 2 nM) to ensure library quality.

Following quality approval, libraries were pooled according to their effective concentrations and desired sequencing data volume, and paired-end 150 bp (PE150) sequencing was performed on the Illumina NovaSeq/Xplus platform to generate 150-bp paired-end reads.

A total of 51 samples were submitted for sequencing, including 25 hypertensive controls and 26 patients with hypertensive intracerebral hemorrhage. Baseline patient characteristics are summarized in Table 1. Box plots illustrated mRNA expression levels based on FPKM values in both groups. Correlation analysis was performed and principal component analysis (PCA) plots were generated (Fig. 1).

Although the variances explained by principal component 1 and principal component 2 were not prominent, the confidence ellipses revealed that the hypertensive intracerebral hemorrhage group exhibited a more scattered distribution, which may reflect heterogeneity among patients secondary to hypertensive intracerebral hemorrhage. In contrast, the non-hemorrhagic hypertensive control group was more tightly clustered, further indicating substantial individual variability in this disease.

These RNA-sequencing data demonstrated that the mRNA expression profile of the hypertensive intracerebral hemorrhage group differed from that of the hypertensive control group, and the differential expression gene (DEG) dataset was reliable. These results ensured the robustness of the subsequent bioinformatic analyses.[11–13]

Table 1
Clinical Characteristics of Patients

Characteristics	ICH Group (n = 26)	Sham Group (n = 25)	P value
Sample	26	25	—
Age	59.3 ± 8.0	60.9 ± 9.0	0.526
Height (cm)	166.7 ± 7.7	165.4 ± 7.6	0.553
Weight (kg)	75.3 ± 8.4	75.0 ± 8.4	0.894
BMI	27.0 ± 1.1	27.3 ± 0.8	0.271
Systolic blood pressure	151.8 ± 5.9	150.8 ± 6.6	0.559
Diastolic blood pressure	91.5 ± 5.2	90.6 ± 5.5	0.561
Gender (male/female, case)	15/11	13/12	0.893
Diabetes (yes/no, case)	9/17	6/19	0.575
Hyperlipidemia (yes/no, case)	19/7	16/9	0.924

1. (A) Expression correlation analysis of samples: Different colors represent the Pearson correlation coefficients. The relationship between correlation coefficients and colors is shown in the legend on the right. A more red color indicates a higher absolute value of the correlation coefficient between samples.
2. (B) FPKM density distribution curve.

(C)box plot of fragments per kilobase of transcript per million mapped reads (FPKM) distribution per sample.

(D) Principal component analysis (PCA) plot of mRNA expression in the two groups. *P < 0.05, **P < 0.01, *P < 0.001.

Identification and Analysis of DEGs

Accordingly, differentially expressed genes (DEGs) were screened out by adopting a significance criterion of false discovery rate (FDR) < 0.01. This threshold was set to guarantee the statistical significance of the obtained results and reduce the probability of false positive findings to the minimum. To gain deeper insights into the potential biological roles and regulatory mechanisms of key genes involved in hypertensive intracerebral hemorrhage, the “clusterProfiler” software package was employed to conduct enrichment analyses of the filtered key genes, including Gene Ontology (GO) and Kyoto Encyclopedia of Genes and Genomes (KEGG) analyses. In the course of the enrichment analysis, only

the enriched terms meeting the significance standard ($P < 0.05$) were retained, which was intended to ensure the dependability and precision of the analytical results.

Primary Neurons, Neural Stem Cells and Other Cell Culture

All animal experimental protocols were approved by the Institutional Animal Care and Use Committee (IACUC) of Shanghai Jiao Tong University. All in vivo animal experiments were performed in strict accordance with the Animal Research: Reporting of In Vivo Experiments (ARRIVE) guidelines and the institutional animal ethical approval document (SYXK2023-026) issued by Shanghai Jiao Tong University. Pregnant female C57BL/6 mice at gestational days 16–18 were purchased from Beijing Leagene Biotechnology Co., Ltd., for subsequent isolation of primary fetal mouse cells. Animals were housed under a standard 12 h light/dark cycle with ad libitum access to standard chow and sterile drinking water. The ambient relative humidity was maintained at 50–60%, and room temperature (RT) was controlled within 18–22°C throughout the feeding period.Pregnant dams were euthanized via gradual carbon dioxide inhalation followed by cervical dislocation to confirm death. Immediately after maternal death, embryonic brains were harvested for isolation of primary neural stem cells.

Primary neurons were isolated from the cerebral cortex and hippocampus of embryonic C57BL/6 mice at embryonic day 16–18 (E16–18), digested with 0.125% trypsin for 5–10 minutes, and then gently dissociated. The resulting suspension was filtered through a 40-μm cell strainer and cultured in Neurobasal medium (21103049, Gibco, USA) supplemented with 2% B27 (17504044, Gibco, USA), 1% GlutaMAX (35050061, Gibco), and 0.5% penicillin-streptomycin. Neurons were counted and seeded onto poly-D-lysine-coated culture plates, and maintained at 37°C in a 5% CO_2 incubator. Half of the culture medium was replenished after 2–3 days, and neurons were used for experiments after 5–7 days of culture.

Mouse neural stem cells (NSCs) were isolated from the cerebral cortex of C57BL/6J mouse embryos at gestational day 16 (G16). Cells were cultured in DMEM/F12 medium (Dulbecco's Modified Eagle Medium/F12, Sigma-Aldrich, Merck KGaA, Darmstadt, Germany) supplemented with 1% B27 supplement (Thermo Fisher Scientific), 20 ng/mL epidermal growth factor (EGF), 20 ng/mL basic fibroblast growth factor (bFGF, PeproTech, Rocky Hill, NJ, USA), and 1% penicillin-streptomycin (Gibco, Thermo Fisher Scientific).

Neurospheres were collected and dissociated into single-cell suspensions using StemPro Accutase cell dissociation reagent (Thermo Fisher Scientific). After resuspension, cells were cultured in suspension to form neurospheres through continuous passaging. To minimize experimental variation, cells at passages 2–4 were used for all experiments.

For differentiation assays, NSCs were seeded at a density of 500 000 cells per well onto poly-D-lysine-coated 24-well plates. After 1–2 days of culture in basal medium, the medium was replaced with Neurobasal medium containing 2% B27 and 1% penicillin-streptomycin.

Human embryonic kidney 293T (HEK293T) cells were purchased from the Cell Bank of the Chinese Academy of Sciences (Shanghai, China) and cultured in high-glucose DMEM (Gibco) supplemented with 10% fetal bovine serum (Gibco) and 1% penicillin-streptomycin (Gibco, Thermo Fisher Scientific). Cells were maintained at 37°C in a humidified incubator with 5% CO_2, and the medium was changed every two days.

Lentiviral Transfection

NSCs were transduced with pSLenti-U6-TuD (mmu-miR-21a-5p)-CMV-EGFP-F2A-Puro-WPRE, pcSLenti-EF1-EGFP-F2A-Puro-CMV-pri-mmu-miR-21a-WPRE, or corresponding control viruses (OBiO Technology, Shanghai, China) at a multiplicity of infection (MOI) of 10. Transduction was performed in a cell culture incubator using fresh complete medium for 24 hours according to the manufacturer's protocol. Transfection efficiency was evaluated by fluorescence microscopy and reverse transcription quantitative polymerase chain reaction (RT-qPCR), and these methods were applied in subsequent in vitro experiments.

Western Blot Analysis

Cell lysates were prepared using radioimmunoprecipitation assay (RIPA) buffer (P0013B, Beyotime). Protein concentrations were quantified using an enhanced BCA protein assay kit. Protein samples (30–50 μg) were separated by 10% sodium dodecyl sulfate-polyacrylamide gel electrophoresis (SDS-PAGE, MB2479, Meilun Biotech, China) and transferred to polyvinylidene difluoride (PVDF) membranes. Membranes were blocked in Tris-buffered saline containing 0.1% Tween-20 and 5% non-fat milk for 90 minutes at room temperature. Subsequently, membranes were incubated with primary antibodies, followed by horseradish peroxidase-conjugated secondary antibodies. Immunoreactive bands were visualized using an ECL Western blot detection kit and imaged with a Bio-Rad imaging system (Bio-Rad, USA). The antibodies used are listed in Table 2.

Table 2
Antibodies for Western blot analysis

Type	Name	Company and product number	Host	Dilution ratio
Primary antibodies	GFAP	Proteintech Cat. no. 16825-1-AP	Rabbit	1:2000
	β-Tubulin III	Cell signaling technology Cat. no 5568S	Rabbit	1:1000
	SOX2	Proteintech Cat. no. 11064-1-AP	Rabbit	1:1000
	β-Actin	Proteintech Cat. no. 20536-1-AP	Mouse	1:4000
	FOS	ABCAM ab208942	Mouse	1:1000
Secondary antibodies	HRP-conjugated Affinipure goat anti-mouse IgG (H + L)	Proteintech Cat. no. SA00001-1	Goat	1:4000
	HRP-conjugated Affinipure goat anti-rabbit IgG (H + L)	Proteintech Cat. no. SA00001-2	Goat	1:2000

Cell viability analysis

Cell viability was measured using an enhanced CCK-8 kit (Beyotime, China). Neurons were separated and cultured in a 24-well plate. Drug were administered after the maturation of neurons, then replenished with fresh medium containing the CCK-8 solution. The absorbance was measured at 450 nm using a BioTek microplate reader after incubation at 37°C for at least 2 h.

RNA extraction, reverse transcription, and RT-qPCR

A TRIzol reagent (Invitrogen, USA) was applied to extract the total RNA from neurons. RNA quantification and assessment of concentration were performed by NanoDrop ND-1000. For cDNA synthesis, 1 μg of extracted total RNA was used and mixed with a PrimeScript RT Reagent Kit (Yeasen, China) to perform reverse transcription. RT-qPCR was performed by a SYBR Green PCR Master Mix (Yeasen, China) with specific primers. The amplification process follows the instructions of the manufacture. β-Actin was used as an internal control for normalization. Specific PCR primers in the experiments are listed in Table 3.

Table 3
Primer sequences for RT-qPCR.

Primer name	Primer sequence
GAPDH	5’-ATCATCAGCAATGCCTCCTG-3’(forward)
	5’-ATGGACTGTGGtcATGAGTC-3’(reverse)
U6	5’-CTCGCTTCGGCAGCACA-3’ (forward)
	5’-AACGCTTCACGAATTTGCGT-3’(reverse)
FOS	5’-CCGGGGATAGCCTCTCTTAC-3’(forward)
	5’-GTGGGAATGAAGTTGGCACT-3’ (reverse)
miR-21	5'-TAGCTTATCAGACTGATGTTGA-3'(forward)
	5'-TAGCTTATCAGACTGATGTTGA-3'(reverse)

Results

Enrichment Analysis of Differentially Expressed Genes in Hypertensive Intracerebral Hemorrhage and Hypertensive Control Subjects

Differential expression analysis was performed between patients with hypertensive intracerebral hemorrhage (HICH) and control subjects. The cutoff thresholds were set as $\log_2$ fold change > 1 for upregulated genes, $\log_2$ fold change < − 1 for downregulated genes, and adjusted p value < 0.05.The expression characteristics of each subject in the two comparisons were represented by a heatmap. (Fig. 2)

The criterion for identification DEGs is FC > 1.5 or FC < 0.67, P < 0.05.

After analyzing the expression profiles of each subject in the two groups, a total of 1564 differentially expressed genes (DEGs) were identified in peripheral blood between HICH patients and hypertensive controls, among which 878 genes were downregulated and 686 genes were upregulated in HICH patients (Fig. 3A).

Functional enrichment analysis of upregulated genes revealed that, compared with the hypertensive control group, peripheral blood cells of HICH patients were enriched in membrane-related cellular components, including the plasma membrane, membrane structures, and nuclear lamina. Enriched molecular functions comprised nuclear receptor signaling transduction and molecular transducer activity, whereas enriched biological processes were mainly concentrated in inflammatory and stress-related responses, including response to external stimulus, defense response, and inflammatory response.

In addition to the pathways mentioned above, downregulated genes were also enriched in the TCR complex, plasma membrane signaling receptor complex, and regulation of multicellular organismal processes, indicating that downregulated genes play important roles in receptor binding and signal transduction.

KEGG pathway analysis showed that upregulated genes in peripheral blood of patients after hemorrhage were enriched in pathways including osteoclast differentiation, Staphylococcus aureus infection, complement and coagulation cascades, neutrophil extracellular trap formation, and cytokine–cytokine receptor interaction. In contrast, downregulated genes were enriched in pathways including cytokine–cytokine receptor interaction, Wnt signaling pathway, signaling pathways regulating pluripotency of stem cells, and pathways in cancer (Figs. 3B–3E).

To identify hub genes among DEGs between HICH and hypertensive control groups, protein–protein interaction (PPI) analysis was conducted. The most highly connected gene nodes were concentrated in the interleukin family, TLR4, IFN-γ, ITGAM, FN1, MMP9, FOS, and CD163, which corroborated the KEGG analysis. These hub DEGs were mainly involved in pathways related to inflammation, immunity, coagulation, and regeneration (Fig. 3F).

Figure 3: Identification and functional enrichment analysis of differentially expressed genes (DEGs) between hypertensive intracerebral hemorrhage and control groups.

(A) Volcano plot showing the distribution of DEGs. The x-axis represents the $\log_2$-transformed fold change (FC), and the y-axis represents the $-\log_{10}$-transformed P-value. Red dots indicate significantly upregulated genes, green dots indicate significantly downregulated genes, and gray dots indicate genes with no significant difference. The criteria for identifying DEGs were $|\log_2 FC| > 1$ and $P < 0.05$.

(B, D) Gene Ontology (GO) enrichment analysis of downregulated (B) and upregulated (D) DEGs. The top enriched terms in biological process (BP), cellular component (CC), and molecular function (MF) categories are presented. The x-axis represents the gene ratio, and the color and size of the dots indicate the $-\log_{10}$(P-value) and the number of genes enriched in each term, respectively.

(C, E) Kyoto Encyclopedia of Genes and Genomes (KEGG) pathway enrichment analysis of downregulated (C) and upregulated (E) DEGs. The x-axis represents the $-\log_{10}$(P-value), and the color gradient indicates the significance of enrichment.

(F) Protein-protein interaction (PPI) network of key DEGs. The size of each node reflects the degree of connectivity, and the edges represent the interactions between proteins.

In Vitro ICH Model

On the basis of our previous sequencing results, we found that peripheral blood RNA from patients after hypertensive intracerebral hemorrhage exhibited gene expression differences compared with hypertensive controls, involving but not limited to inflammation, immunity, and regeneration. To further

verify the function of the key hub gene FOS, we aimed to simulate the intracerebral hemorrhage environment in vitro and established a hemin-induced primary neuron injury model.

After 24 hours of treatment, cell viability was evaluated at different hemin concentrations. The results showed that cell viability decreased in a concentration-dependent manner with increasing hemin levels. To quantify the expression level of FOS in neurons, mRNA levels of FOS were detected by RT-qPCR. We found that FOS expression was significantly increased in this in vitro hemorrhagic model compared with the control group.

Detection of FOS in Neural Stem Cells

Neural stem cells (NSCs) were isolated and cultured from fetal mouse brains, and the purity of isolated NSCs was verified by immunofluorescence (Fig. 4D). The isolated NSCs were capable of proliferating and forming neurospheres (Fig. 4C). After switching to differentiation-inducing medium, their ability to differentiate and mature into neurons and glial cells was confirmed (Fig. 4E), ensuring their suitability for subsequent experiments.

To clarify the role of FOS in the biological behavior of NSCs, RT-qPCR was performed on days 1, 3, 5, and 7 during NSC neuronal differentiation. The results showed that intracellular FOS levels increased in a time-dependent manner. Western blot analysis simultaneously confirmed a consistent trend at the protein level, suggesting that FOS may promote the differentiation of neural stem cells.

Figure4: Isolation, Culture, and Related Assays of Neural Stem Cells

1. (A) Cell viability assay showing the effects of different concentrations of hemin (0, 25, 50, 75, 100 μM) on neuronal cell viability.
2. (B) Relative expression level of FOS in the hemin-treated group versus the control group (normalized to GAPDH).
3. (C) Representative image of neural stem cell spheres.

(D-E) Immunofluorescence staining of cell markers. (D) DAPI (blue), FOS (green), and merged image; (E) DAPI (blue), Tuj1 (green)/GFAP (green)/MBP (red), and merged images, showing the expression of different lineage markers during differentiation.

1. (F) Quantitative analysis of FOS expression in neural stem cells at different time points after differentiation (Days 1, 3, 5, and 7).
2. (G) Western blot analysis of FOS protein levels on Day 1 and Day 7, with GAPDH as the internal reference.
3. (H) Relative protein expression of FOS in neural stem cells on Day 1 versus Day 7 after differentiation (normalized to GAPDH).

Combined with previous studies from our group and other researchers (analyzed in detail in the Discussion section), relationships exist among miR-21, FOS, and SOX2. We constructed a miR-21 overexpression lentivirus and verified its transfection efficiency by RT-qPCR (Fig. 5A). Subsequently, the expression levels of SOX2 and FOS were detected after lentiviral transfection. The results indicated that miR-21 overexpression reduced SOX2 expression but increased FOS expression (Figs. 5B–5E), and vice versa.

Furthermore, NSCs were transfected with SOX2-related lentiviruses to manipulate SOX2 expression levels (Figs. 5F–5G). Detection of FOS protein revealed that FOS was significantly upregulated when SOX2 was inhibited, whereas FOS expression was decreased upon SOX2 overexpression (Figs. 5H–5I).

(A) qRT-PCR analysis showing the relative expression level of miR-21 in cells treated with LV-anti-miR-21, LV-miR-21, or LV-NC (normalized to U6).

(B, D) Western blot analysis showing the protein levels of FOS (B) and SOX2 (D) in cells treated with LV-miR-21, LV-NC, or LV-anti-miR-21, with GAPDH as the loading control.

(C, E) Quantitative analysis of the relative protein expression of FOS (C) and SOX2 (E) in the three groups.

(F, H) Western blot analysis showing the protein levels of SOX2 (F) and FOS (H) in cells treated with LV-SOX2, LV-NC, or LV-anti-SOX2, with GAPDH as the loading control.

(G, I) Quantitative analysis of the relative protein expression of SOX2 (G) and FOS (I) in the three groups.

Discussion

Intracerebral hemorrhage (ICH) is a cerebrovascular disease with high mortality. In this study, we conducted a comprehensive transcriptomic analysis of ICH patients and control subjects to elaborate on the molecular basis of hypertensive intracerebral hemorrhage (HICH). Through biological analysis, we identified several genes and pathways with differential expression between HICH patients and hypertensive controls, which provides a foundation for further understanding the complex biological processes of this disease and offers insights for in-depth exploration of subsequent treatment strategies.

In the biological analysis of RNA-seq data, we screened 878 downregulated genes and 686 upregulated genes. GO enrichment analysis showed that most differentially expressed genes (DEGs) are involved in inflammation, immune stress, and self-protection. KEGG pathway enrichment analysis indicated that DEGs may be involved in pathways closely related to inflammation, complement and coagulation cascades, cytokine-cytokine receptor binding, and regulation of stem cell pluripotency. These components support that the screened DEGs are mainly associated with immune system activation, as well as other inflammatory, cell proliferation, and regeneration processes. Next, we will focus on the hub genes in the protein-protein interaction (PPI) network to identify important nodes in the pathological process of ICH and potential targets for subsequent treatment.

In the pathological process of ICH, our sequencing results suggest that the interleukin (IL) family plays a pivotal role, among which IL-1β, IL-10, and IL-8 are particularly significant. Consistent with our findings, a study on a rat model of ICH showed that interleukin-1β (IL-1β), a pro-inflammatory cytokine, is elevated in the serum after HICH and is positively correlated with the degree of cerebral edema following ICH.[14] In a clinical trial, researchers inhibited IL-1 expression using an IL-1 receptor antagonist, which reduced in vivo inflammatory levels in the short term compared with the control group. However, this trial lacked specific evaluation of cerebral edema severity and long-term control of inflammatory levels; further confirmation of the safety and efficacy of IL-1 inhibitors requires a larger study scale, longer-term observation indicators, and more rigorous trial design.[15] Similar to IL-1, IL-8 is also closely associated with ICH: in 94 patients with basal ganglia ICH, IL-8 was positively correlated with the severity of cerebral edema ($r = 0.305$, $p < 0.05$).[16, 17]In contrast to IL-1, IL-8 inhibitors have been applied in animal models and clinical trials of ischemic stroke. Inhibition of IL-8 as a therapeutic target for stroke has been studied, including the use of antiplatelet agents to inhibit IL-8 in patients with ischemic stroke,[18] and the use of the IL-8 inhibitor reparixin to reduce inflammation and neurological dysfunction in rats with transient cerebral ischemia.[19]In a rabbit model of cerebral ischemia treated with an IL-8 neutralizing antibody, edema and infarct size were reduced[20]. Unlike other cytokines whose expression changes significantly after ICH, IL-10 is a key anti-inflammatory cytokine that can inhibit pro-inflammatory signals and immune responses after ICH. Previous studies have shown that IL-10-deficient mice exhibit more severe neuroinflammation, cerebral edema, iron deposition, and neurological deficits after ICH, which are mainly associated with delayed hematoma clearance.[21]Moreover, peripheral IL-10 helps alleviate blood-brain barrier (BBB) damage and neurobehavioral deficits after ICH by regulating the IL-10R/JAK1/STAT3 signaling axis.[22]Therefore, the expression of the IL family in peripheral blood can directly affect the inflammatory level and cerebral edema degree after ICH, but the roles of individual members may be completely opposite. Therapeutic attempts targeting the IL family mainly focus on inflammation, cerebral edema, and BBB damage after ICH. However, future studies are needed to further clarify the expression trends and functional directions of all IL family members throughout the entire pathological course of ICH, thereby targeting and verifying potential biomarkers and therapeutic targets centered on IL family members.

Among other hub genes, most are related to cellular immunity, such as some leukocyte differentiation antigens (CD163, CD11b, CD284, etc.). Next, we will sort out and summarize the roles of these immunity-related genes in ICH. CD163 is a scavenger receptor that promotes monocyte binding and endocytosis of hemoglobin-haptoglobin complexes, reducing the cytotoxic load of free hemoglobin after tissue hemorrhage.[23, 24] Studies have found that CD163 may play a key role in limiting inflammation and inhibiting secondary damage after hemorrhagic injury.[25, 26]Clinical studies have shown that low levels of CD163 in serum and cerebrospinal fluid are of great significance for identifying patients with increased acute hematoma volume, expansion of perihematomal edema, and poor short-term prognosis.[27]Further studies thereafter suggested that FKN can enhance erythrophagocytosis of microglia in vitro by regulating the CD163/heme oxygenase-1 (HO-1) axis.[28] TLR4, full name Toll-like receptor 4 (also known

as CD284), is one of the widely studied molecular receptors in ICH. TLR4 is expressed in various cell types in the central nervous system, including microglia, neurons, and astrocytes, as well as in peripheral blood cells such as leukocytes, macrophages, and platelets.[29–33]After ICH, TLR4 mRNA and protein expression increase significantly. Although ICH induces upregulation of TLR4 expression in neurons, astrocytes, and microglia, TLR4 is mainly expressed in CD11b-positive microglia in mice.[30]Therefore, CD11b and TLR4 should have consistent functional directions. Studies have found that TLR4 signaling on microglia triggers inflammatory damage caused by ICH, leading to the release of inflammatory cytokines and infiltration of neutrophils.[31, 34] In addition, the release of IL-8 (i.e., CXCL8) mentioned above is dependent on TLR4 expression during inflammation, so TLR4 connects many inflammation-inducing genes and pathways.[35]Since TLR4 signaling plays an important role in inflammatory damage caused by ICH, inhibition of TLR4 should be beneficial for reducing inflammation and neural damage after ICH. Therefore, further searching for antagonists that block TLR4 and CD11b and evaluating their efficacy is the mainstream direction in the future. In other studies, the proportion of neutrophils among immune cell types in ICH patients is higher than that of other immune cells, which leads to secondary tissue damage such as inflammation.[36]Therefore, cell apoptosis and cytotoxicity caused by inflammation are not limited to secondary damage in the brain. Finding potential biomarkers of associated leukocytes that can stably change after ICH, and searching for their antagonists or agonists to inhibit inflammation have become the current top priorities.

FOS (Fos Proto-Oncogene, AP-1 Transcription Factor Subunit), commonly known as c-Fos, is a prototype member of the well-known "Immediate Early Gene (IEG)" family. The proto-oncogene c-Fos encodes a transcription factor that plays a key role in cell proliferation, differentiation, and apoptosis.[37, 38]In this study, the expression level of c-Fos within 24 hours after ICH showed an increasing trend compared with the control group. Therefore, we cultured primary neuronal cells and added hemin to simulate the in vitro ICH environment. Cell viability testing showed that the cell viability of the experimental group was significantly lower than that of the control group. Determination of c-Fos levels in the two groups of cells revealed that neurons treated with hemin had higher c-Fos expression. These results are consistent with previous animal studies, in which researchers revealed that c-Fos may be associated with neuronal apoptosis in a rat ICH model, and the FasL/Fas-mediated apoptotic pathway may be involved in this process in both in vivo and in vitro experiments.[37]In other destructive intracerebral diseases, such as traumatic brain injury and ischemic stroke, rapid activation of c-Fos has also been detected in the cerebral cortex.[39–42] At the same time, we also noted that some studies focus more on the role of c-Fos in cell proliferation and differentiation. Under most conditions, c-Fos is considered necessary for the exponential growth phase of the cell cycle and is an important inducer of cell proliferation.[43, 44]In our previous studies, we found that transplantation of neural stem cells (NSCs) after ICH may activate endogenous NSCs to promote neurological function recovery. Therefore, we wondered whether the FOS gene can play a role in NSCs. We tentatively cultured primary NSCs and verified their good proliferation and differentiation abilities. During the induction of their differentiation into neurons, we detected the expression level of c-Fos in the samples, and the results showed that the expression level of c-Fos

increased correspondingly with the increase of differentiation time and degree. Western blot analysis of samples on the first and seventh days of differentiation further confirmed this point. Therefore, we believe that c-Fos is involved in the differentiation process of NSCs. Our research group has previously conducted detailed studies on the role of miR-21 and SOX2 in the proliferation and differentiation of NSCs, and found that miR-21 can regulate the proliferation and differentiation ability of NSCs by targeting the SOX2/LIN28-let-7 signaling pathway. However, the problem is that when we knocked down SOX2 expression, we also impaired the normal differentiation ability of NSCs.[45]We reviewed relevant literature and found that SOX2 is crucial for maintaining the long-term self-renewal and normal differentiation ability of NSCs.[46, 47] At the same time, researchers found that Fos can rescue the long-term proliferation ability of SOX2-deficient NSCs.[48] In terms of differentiation, another study suggested that re-transduction of Fos into SOX2-deficient NSCs confers the ability to differentiate into neuronal precursors, but further maturation remains to be further explored and studied.[49]Therefore, we wondered whether c-Fos is involved in the regulatory pathway of miR-21 and SOX2. We constructed lentiviruses overexpressing and silencing miR-21 and transfected them into NSCs. After verifying their infection efficiency, we detected the expression levels of SOX2 and c-Fos by Western blot. We found that SOX2 is inhibited by miR-21, while c-Fos maintains the same expression trend as miR-21. Studies have shown through bioinformatics and luciferase experiments that in glioma cells, miR-181b regulates FOS expression by directly targeting the binding site in the 3'UTR, and the decrease of FOS inhibits miR-21 expression by binding to the miR-21 promote.[50]In addition, researchers found that as a key regulator of cell proliferation, apoptosis, tumor invasiveness, and angiogenesis, the transcription factor AP-1 is mainly formed by dimerization between members of the JUN and FOS protein families.[51, 52] PDCD4 acts as a negative regulator of AP-1, and miR-21-mediated downregulation of PDCD4 is crucial for the maximal induction of AP-1 activity under RAS signal stimulation. This study found that miR-21 is not only controlled by AP-1 but also a necessary condition for the maximal induction of AP-1 activity, serving as both a target and a regulator of the AP-1 complex.[53]Therefore, the interaction between c-Fos and miR-21 is complex, but it has not been fully studied in other nervous system diseases except tumors. Therefore, in view of various evidences suggesting that the role of c-Fos in ICH is not limited to cell apoptosis, and experiments have confirmed that c-Fos has the potential to participate in proliferation and differentiation in NSCs, we believe this is worthy of further study. In addition, our experiments verified that SOX2 can inhibit FOS expression. In SOX2-del NSCs, overexpression of Fos can stimulate the initial neuronal differentiation of bipotent neuronal/glial precursors but fails to induce more advanced neuronal differentiation programs. In the absence of SOX2, NSC differentiation often stops at the level of bipotent glial/neuronal precursors; by overexpressing Fos, cells may be diverted from the glial fate to the neuronal fate, and some of these cells may initiate correct neuronal differentiation.[49]FOS assumes part of the functions of SOX2 but cannot completely replace it. Combined with relevant literature suggesting that Fos is a direct target of SOX2 itself.[48, 54]We believe that further verifying the binding mode and regulatory mechanism between FOS and SOX2 is crucial for further understanding the role of miR-21 in regulating the biological processes of NSCs.

This study has several limitations that need to be acknowledged. First, the HICH patients and hypertensive controls selected in our study were all relatively old, while ICH is currently tending to be younger, which may lead to deviations between our sequencing results and the actual situation. Second, due to physical conditions, the elderly have a higher incidence of tumors and other diseases, so the sequencing results may be mixed with the effects of some other undiscovered diseases. Therefore, in subsequent studies, expanding the sample size, collecting continuous blood samples earlier and for a longer duration before symptom onset, analyzing matched control groups, and adding whole-transcriptome sequencing and result analysis to the transcriptome will further improve the understanding of the pathophysiological mechanism of ICH and help find reliable therapeutic targets. Second, more experiments are needed to verify the potential molecular mechanisms of DEGs. Although our experiments confirmed the correlation between miR-21, SOX2, and c-Fos, there is still a lack of exploration of molecular-level mechanisms. Therefore, in subsequent studies, we can verify the interaction between DNA, RNA, and proteins through more experimental methods such as RIP, CO-IP, and CHIP-seq, and further extend these studies to animal experiments.

Conclusion

Collectively, RNA sequencing (RNA-seq) effectively captured and delineated the precise transcriptional profiles and differential expression changes in the peripheral blood samples obtained from patients with hypertensive intracerebral hemorrhage, in contrast to those from hypertensive control individuals without intracerebral hemorrhage. This transcriptional profiling not only reveals the distinct molecular signatures associated with hypertensive intracerebral hemorrhage but also provides valuable clues regarding the systemic molecular perturbations and pathological processes underlying this disease. Importantly, the findings derived from the present study identify and establish a potential therapeutic target that is centered on the FOS gene, with the specific purpose of activating neural stem cells in the post-intracerebral hemorrhage phase. Neural stem cell activation plays a critical role in facilitating neural regeneration, repairing damaged brain tissue, and improving neurological function recovery after intracerebral hemorrhage, which are key factors in alleviating the long-term neurological deficits caused by this devastating condition. Moreover, the identification of the FOS gene as a candidate therapeutic target offers a novel direction for the development of targeted interventions, potentially addressing the unmet clinical needs in the treatment and management of hypertensive intracerebral hemorrhage. These results also lay a solid foundation for future in vitro and in vivo studies to further validate the regulatory role of the FOS gene in neural stem cell activation and explore its clinical translational potential in improving patient outcomes.

Declarations

Conflict of interest statement

The authors declare no conflict of interest.

Data Availability Statement

The raw sequence data reported in this paper have been deposited in the GEO database(GSE335924).

Funding information

This work was supported by Shanghai Minhang District Health Commission Project (2022MHZ062)

Clinical trail number：not applicable

References

1. Global regional, and national burden of stroke and its risk factors, 1990–2019: a systematic analysis for the Global Burden of Disease Study 2019 [J]. *Lancet Neurol.* **20** (10), 795–820 (2021).
2. LAWES C M, F. E. I. G. I. N. V. L. et al. Worldwide stroke incidence and early case fatality reported in 56 population-based studies: a systematic review [J]. *Lancet Neurol.* **8** (4), 355–369 (2009).
3. AN, S. J., KIM T J, YOON, B. W. & Epidemiology Risk Factors, and Clinical Features of Intracerebral Hemorrhage: An Update [J]. *J. Stroke*. **19** (1), 3–10 (2017).
4. CAO, S. et al. Hematoma Changes During Clot Resolution After Experimental Intracerebral Hemorrhage [J]. *Stroke* **47** (6), 1626–1631 (2016).
5. XI, G. & KEEP R F, HOFF, J. T. Mechanisms of brain injury after intracerebral haemorrhage [J]. *Lancet Neurol.* **5** (1), 53–63 (2006).
6. ZIAI W C. Hematology and inflammatory signaling of intracerebral hemorrhage [J]. *Stroke* **44** (6 Suppl 1), S74–S78 (2013).
7. ZHU, H. & WANG, Z. Role and mechanisms of cytokines in the secondary brain injury after intracerebral hemorrhage [J]. *Prog Neurobiol.* **178**, 101610 (2019).
8. XUE, M. Neuroinflammation in intracerebral haemorrhage: immunotherapies with potential for translation [J]. *Lancet Neurol.* **19** (12), 1023–1032 (2020).
9. HEMPHILL, J. C. 3RD et al. Guidelines for the Management of Spontaneous Intracerebral Hemorrhage: A Guideline for Healthcare Professionals From the American Heart Association/American Stroke Association [J]. *Stroke* **46** (7), 2032–2060 (2015).
10. CHEN, S. et al. An update on inflammation in the acute phase of intracerebral hemorrhage [J]. *Transl Stroke Res.* **6** (1), 4–8 (2015).
11. KANEHISA, M. KEGG: kyoto encyclopedia of genes and genomes [J]. *Nucleic Acids Res.* **28** (1), 27–30 (2000).
12. KANEHISA M. Toward understanding the origin and evolution of cellular organisms [J]. *Protein science: publication Protein Soc.* **28** (11), 1947–1951 (2019).
13. KANEHISA, M. et al. KEGG: biological systems database as a model of the real world [J]. *Nucleic Acids Res.* **53** (D1), D672–d7 (2025).

14. WEI, P. et al. Correlation between serum IL-1beta levels and cerebral edema extent in a hypertensive intracerebral hemorrhage rat model [J]. *Neurol. Res.* **36** (2), 170–175 (2014).
15. PARRY-JONES A R, STOCKING K, MACLEOD, M. J. et al. Phase II randomised, placebo-controlled, clinical trial of interleukin-1 receptor antagonist in intracerebral haemorrhage: BLOcking the Cytokine IL-1 in ICH (BLOC-ICH) [J]. *Eur. Stroke J.* **8** (3), 819–827 (2023).
16. WANG X M et al. Expressions of serum inflammatory cytokines and their relationship with cerebral edema in patients with acute basal ganglia hemorrhage [J]. *Eur. Rev. Med. Pharmacol. Sci.* **20** (13), 2868–2871 (2016).
17. WALSH K B, ZHANG, X. et al. Intracerebral Hemorrhage Induces Inflammatory Gene Expression in Peripheral Blood: Global Transcriptional Profiling in Intracerebral Hemorrhage Patients [J]. *DNA Cell. Biol.* **38** (7), 660–669 (2019).
18. AL-BAHRANI A, TAHA, S. et al. TNF-alpha and IL-8 in acute stroke and the modulation of these cytokines by antiplatelet agents [J]. *Curr. Neurovasc Res.* **4** (1), 31–37 (2007).
19. VILLA, P. et al. CAVALIERI B,. The interleukin-8 (IL-8/CXCL8) receptor inhibitor reparixin improves neurological deficits and reduces long-term inflammation in permanent and transient cerebral ischemia in rats [J]. Mol Med, 13(3–4): 125 – 33. (2007).
20. MATSUMOTO, T. et al. Prevention of cerebral edema and infarct in cerebral reperfusion injury by an antibody to interleukin-8 [J]. *Lab. Invest.* **77** (2), 119–125 (1997).
21. LI, Q. et al. Microglia-derived interleukin-10 accelerates post-intracerebral hemorrhage hematoma clearance by regulating CD36 [J]. *Brain Behav. Immun.* **94**, 437–457 (2021).
22. XU, Y. et al. Peripheral cytokine interleukin-10 alleviates perihematomal edema after intracerebral hemorrhage via interleukin-10 receptor/JAK1/STAT3 signaling [J]. *CNS Neurosci. Ther.* **30** (6), e14796 (2024).
23. THOMSEN, J. H. et al. The haptoglobin-CD163-heme oxygenase-1 pathway for hemoglobin scavenging [J]. Oxid Med Cell Longev, 2013: 523652. (2013).
24. BUECHLER, C. et al. Regulation of scavenger receptor CD163 expression in human monocytes and macrophages by pro- and antiinflammatory stimuli [J]. *J. Leukoc. Biol.* **67** (1), 97–103 (2000).
25. SCHAER C, A. et al. Constitutive endocytosis of CD163 mediates hemoglobin-heme uptake and determines the noninflammatory and protective transcriptional response of macrophages to hemoglobin [J]. *Circ. Res.* **99** (9), 943–950 (2006).
26. KRISTIANSEN, M. et al. Identification of the haemoglobin scavenger receptor [J]. *Nature* **409** (6817), 198–201 (2001).
27. ROY-O'REILLY M, Z. H. U. L. et al. Soluble CD163 in intracerebral hemorrhage: biomarker for perihematomal edema [J]. *Ann. Clin. Transl Neurol.* **4** (11), 793–800 (2017).
28. YOU, M. et al. Neuron derived fractalkine promotes microglia to absorb hematoma via CD163/HO-1 after intracerebral hemorrhage [J]. *Cell. Mol. Life Sci.* **79** (5), 224 (2022).

29. KIELIAN T. Toll-like receptors in central nervous system glial inflammation and homeostasis [J]. *J. Neurosci. Res.* **83** (5), 711–730 (2006).
30. LIN, S. et al. Heme activates TLR4-mediated inflammatory injury via MyD88/TRIF signaling pathway in intracerebral hemorrhage [J]. *J. Neuroinflammation*. **9**, 46 (2012).
31. MA C X et al. Toll-like receptor 4/nuclear factor-kappa B signaling detected in brain after early subarachnoid hemorrhage [J]. *Chin. Med. J. (Engl)*. **122** (13), 1575–1581 (2009).
32. SMILEY S T & KING J A HANCOCK W W. Fibrinogen stimulates macrophage chemokine secretion through toll-like receptor 4 [J]. *J. Immunol.* **167** (5), 2887–2894 (2001).
33. ARAVALLI R N, PETERSON P K, LOKENSGARD, J. R. Toll-like receptors in defense and damage of the central nervous system [J]. *J. Neuroimmune Pharmacol.* **2** (4), 297–312 (2007).
34. TENG, W. et al. Activation of TLR4-mediated NFkappaB signaling in hemorrhagic brain in rats [J]. Mediators Inflamm, 2009: 473276. (2009).
35. HENRICKS P A, M. O. R. T. A. Z. E. et al. Cigarette smoke induces the release of CXCL-8 from human bronchial epithelial cells via TLRs and induction of the inflammasome [J]. *Biochim. Biophys. Acta*. **1812** (9), 1104–1110 (2011).
36. DU, Y. et al. Comprehensive insight on immune landscape in intracerebral hemorrhage patients with single-cell RNA sequencing: from blood to hematoma [J]. *J. Neuroinflammation*. **22** (1), 195 (2025).
37. CHEN, X. et al. Up-regulation of c-Fos associated with neuronal apoptosis following intracerebral hemorrhage [J]. *Cell. Mol. Neurobiol.* **35** (3), 363–376 (2015).
38. LARA APARICIO S Y et al. Current Opinion on the Use of c-Fos in Neuroscience [J]. *NeuroSci* **3** (4), 687–702 (2022).
39. HATA, R. & MAEDA, K. Dynamics of regional brain metabolism and gene expression after middle cerebral artery occlusion in mice [J]. *J. Cereb. Blood Flow. Metab.* **20** (2), 306–315 (2000).
40. NAGY, Z. [Regulatory mechanisms in focal cerebral ischemia. New possibilities in neuroprotective therapy] [J]. *Ideggyogy Sz.* **55** (3–4), 73–85 (2002).
41. NIU, Q. et al. The effect of c-Fos demethylation on sodium fluoride-induced apoptosis in L-02 cells [J]. *Biol. Trace Elem. Res.* **149** (1), 102–109 (2012).
42. SHARMA, H. S. et al. Spinal cord injury induced c-fos expression is reduced by p-CPA, a serotonin synthesis inhibitor. An experimental study using immunohistochemistry in the rat [J]. *Acta Neurochir. Suppl.* **76**, 297–301 (2000).
43. PAI, S. R. BIRD R C. c-fos expression is required during all phases of the cell cycle during exponential cell proliferation [J]. Anticancer Res, 14(3a): 985 – 94. (1994).
44. SHAULIAN, E. AP-1 in cell proliferation and survival [J]. *Oncogene* **20** (19), 2390–2400 (2001).
45. DAI, W. et al. Transplanting neural stem cells overexpressing miRNA-21 can promote neural recovery after cerebral hemorrhage through the SOX2/LIN28-let-7 signaling pathway [J]. *Anim. Model. Exp. Med.* **8** (10), 1760–1774 (2025).

46. MERCURIO, S., SERRA, L. & NICOLIS S K.. More than just Stem Cells: Functional Roles of the Transcription Factor Sox2 in Differentiated Glia and Neurons [J]. *Int. J. Mol. Sci.*, **20**(18). (2019).
47. CIMADAMORE, F. et al. SOX2-LIN28/let-7 pathway regulates proliferation and neurogenesis in neural precursors [J]. *Proc. Natl. Acad. Sci. U.S.A.* **110** (32), E3017–E3026 (2013).
48. PAGIN, M. et al. Sox2 controls neural stem cell self-renewal through a Fos-centered gene regulatory network [J]. *Stem cells (Dayton Ohio)*. **39** (8), 1107–1119 (2021).
49. PAGIN, M. et al. FOS Rescues Neuronal Differentiation of Sox2-Deleted Neural Stem Cells by Genome-Wide Regulation of Common SOX2 and AP1(FOS-JUN) Target Genes [J]. *Cells*, **10**(7). (2021).
50. TAO, T. et al. Involvement of FOS-mediated miR-181b/miR-21 signalling in the progression of malignant gliomas [J]. *Eur. J. Cancer*. **49** (14), 3055–3063 (2013).
51. SHAULIAN, E. AP-1 as a regulator of cell life and death [J]. *Nat. Cell. Biol.* **4** (5), E131–E136 (2002).
52. EFERL, R. & WAGNER E F. AP-1: a double-edged sword in tumorigenesis [J]. *Nat. Rev. Cancer*. **3** (11), 859–868 (2003).
53. TALOTTA, F. et al. An autoregulatory loop mediated by miR-21 and PDCD4 controls the AP-1 activity in RAS transformation [J]. *Oncogene* **28** (1), 73–84 (2009).
54. BERTOLINI, J. A. et al. Mapping the Global Chromatin Connectivity Network for Sox2 Function in Neural Stem Cell Maintenance [J]. *Cell. stem cell.*, **24**(3): (2019). 462 – 76.e6.

Figures

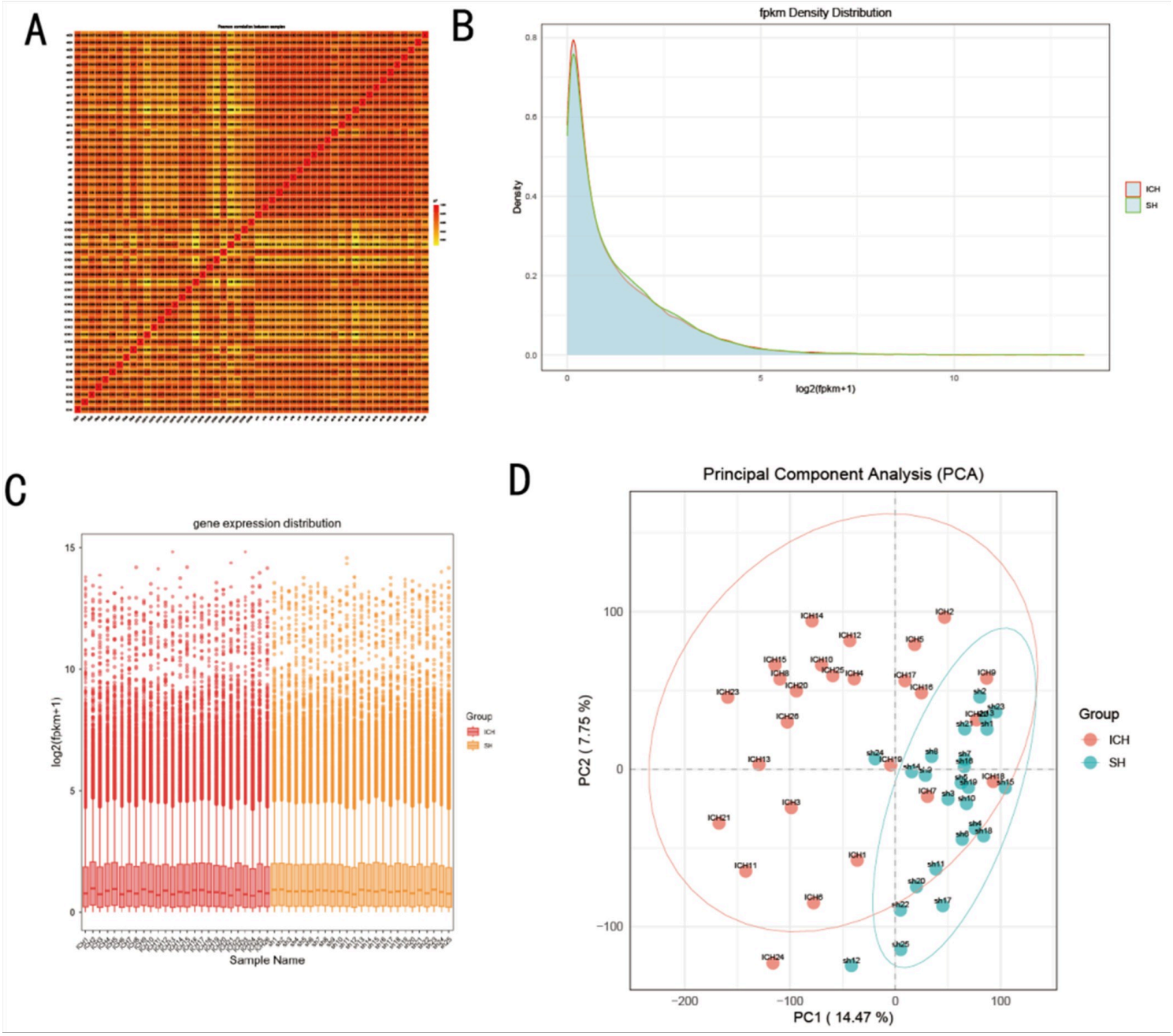


Figure 1

Correlation, distribution, and principal component analysis of gene expression in two groups.

(A) Expression correlation analysis of samples: Different colors represent the Pearson correlation coefficients. The relationship between correlation coefficients and colors is shown in the legend on the right. A more red color indicates a higher absolute value of the correlation coefficient between samples.

(B) FPKM density distribution curve.

(C)box plot of fragments per kilobase of transcript per million mapped reads (FPKM) distribution per sample.

(D) Principal component analysis (PCA) plot of mRNA expression in the two groups. *P < 0.05, **P < 0.01, *P < 0.001.

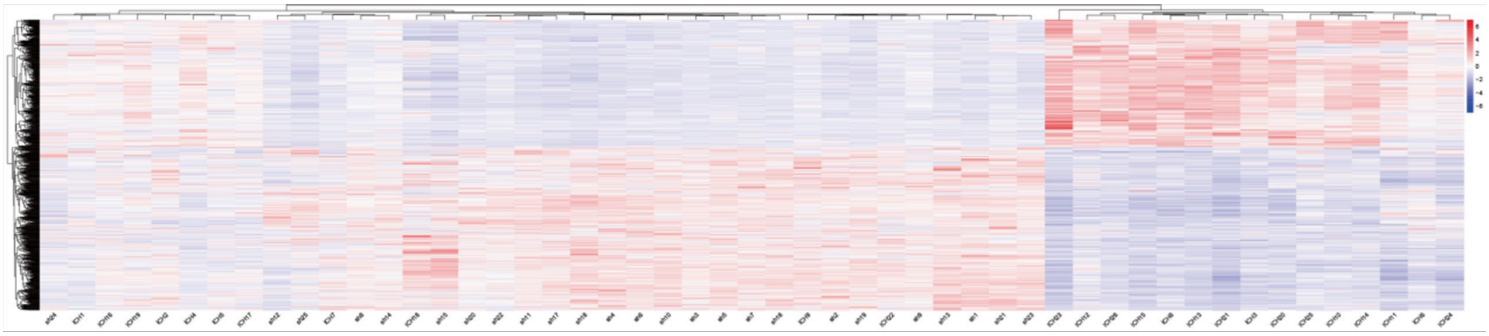


Figure 2

Heatmaps of comparisons of gene expression.

The criterion for identification DEGs is FC > 1.5 or FC < 0.67, P < 0.05.

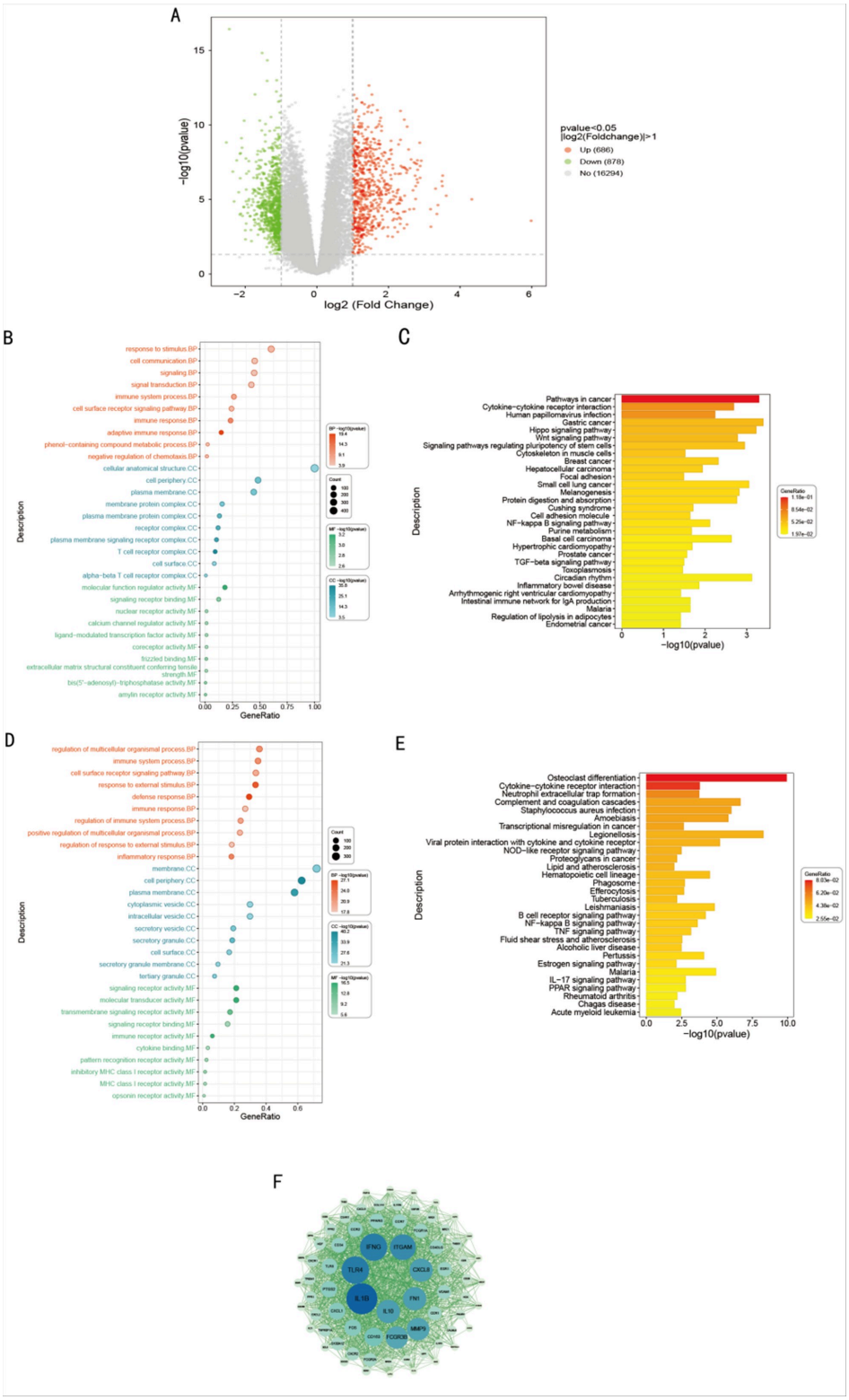


Figure 3

Identification and functional enrichment analysis of differentially expressed genes (DEGs) between hypertensive intracerebral hemorrhage and control groups.

(A) Volcano plot showing the distribution of DEGs. The x-axis represents the $\log_2$-transformed fold change (FC), and the y-axis represents the $-\log_{10}$-transformed P-value. Red dots indicate significantly

upregulated genes, green dots indicate significantly downregulated genes, and gray dots indicate genes with no significant difference. The criteria for identifying DEGs were $|\log_2 FC| > 1$ and $P < 0.05$.

(B, D) Gene Ontology (GO) enrichment analysis of downregulated (B) and upregulated (D) DEGs. The top enriched terms in biological process (BP), cellular component (CC), and molecular function (MF) categories are presented. The x-axis represents the gene ratio, and the color and size of the dots indicate the $-\log_{10}$(P-value) and the number of genes enriched in each term, respectively.

(C, E) Kyoto Encyclopedia of Genes and Genomes (KEGG) pathway enrichment analysis of downregulated (C) and upregulated (E) DEGs. The x-axis represents the $-\log_{10}$(P-value), and the color gradient indicates the significance of enrichment.

(F) Protein-protein interaction (PPI) network of key DEGs. The size of each node reflects the degree of connectivity, and the edges represent the interactions between proteins.

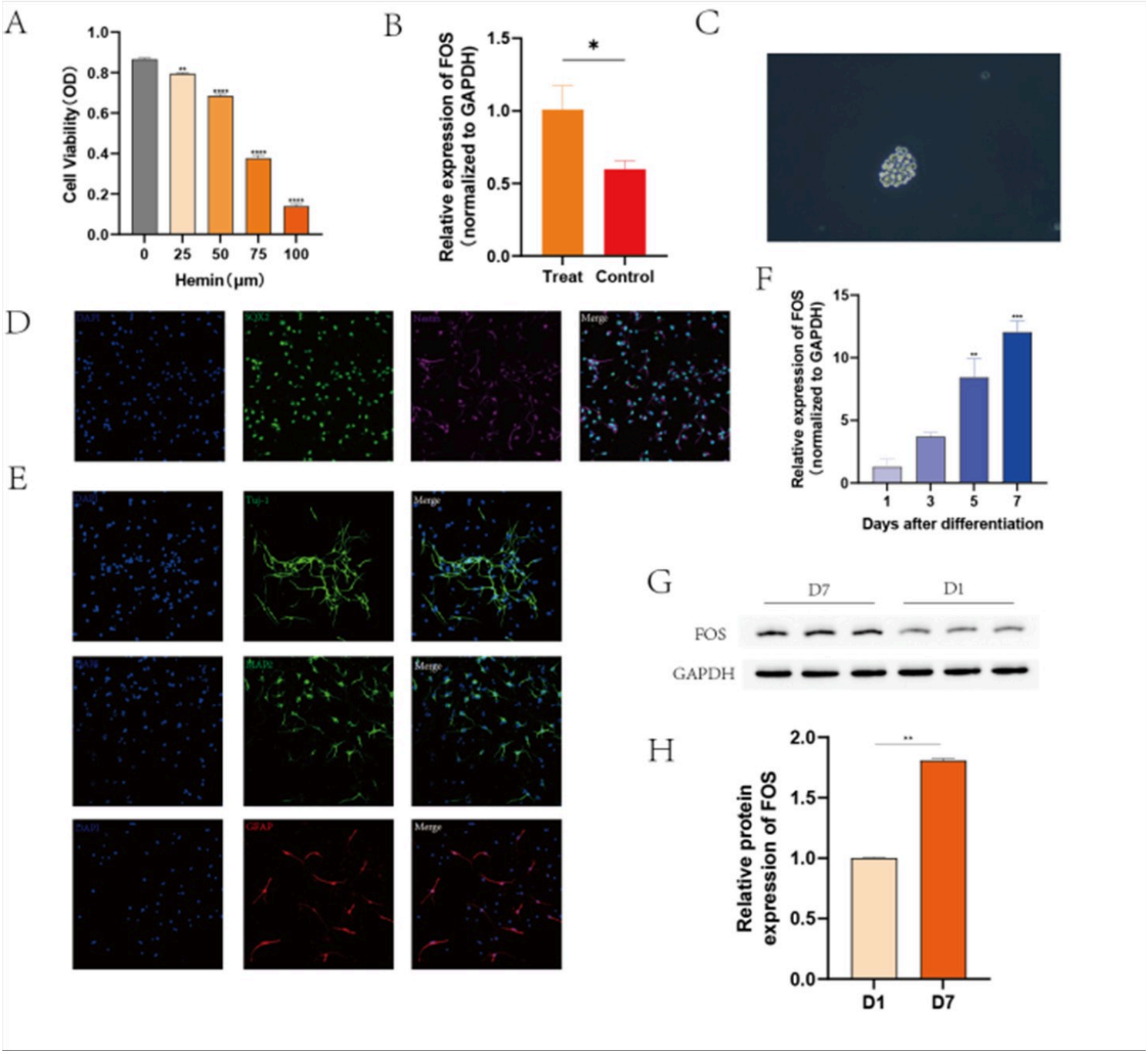


Figure 4

Isolation, Culture, and Related Assays of Neural Stem Cells

(A) Cell viability assay showing the effects of different concentrations of hemin (0, 25, 50, 75, 100 μM) on neuronal cell viability.

(B) Relative expression level of FOS in the hemin-treated group versus the control group (normalized to GAPDH).

(C) Representative image of neural stem cell spheres.

(D-E) Immunofluorescence staining of cell markers. (D) DAPI (blue), FOS (green), and merged image; (E) DAPI (blue), Tuj1 (green)/GFAP (green)/MBP (red), and merged images, showing the expression of different lineage markers during differentiation.

(F) Quantitative analysis of FOS expression in neural stem cells at different time points after differentiation (Days 1, 3, 5, and 7).

(G) Western blot analysis of FOS protein levels on Day 1 and Day 7, with GAPDH as the internal reference.

(H) Relative protein expression of FOS in neural stem cells on Day 1 versus Day 7 after differentiation (normalized to GAPDH).

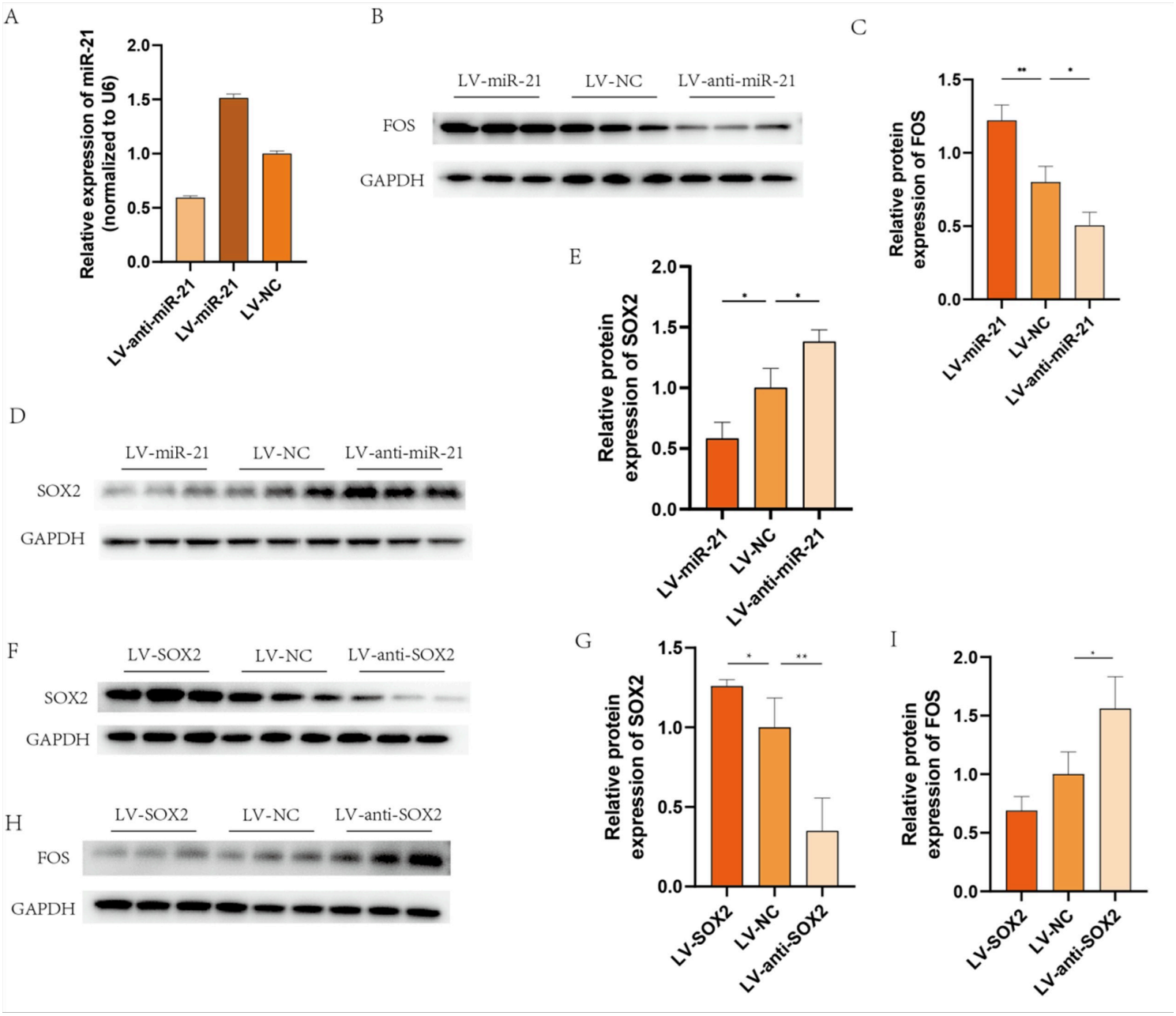


Figure 5

Regulatory relationship among miR-21, SOX2, and FOS in neural stem cells.

(A) qRT-PCR analysis showing the relative expression level of miR-21 in cells treated with LV-anti-miR-21, LV-miR-21, or LV-NC (normalized to U6).

(B, D) Western blot analysis showing the protein levels of FOS (B) and SOX2 (D) in cells treated with LV-miR-21, LV-NC, or LV-anti-miR-21, with GAPDH as the loading control.

(C, E) Quantitative analysis of the relative protein expression of FOS (C) and SOX2 (E) in the three groups.

(F, H) Western blot analysis showing the protein levels of SOX2 (F) and FOS (H) in cells treated with LV-SOX2, LV-NC, or LV-anti-SOX2, with GAPDH as the loading control.

(G, I) Quantitative analysis of the relative protein expression of SOX2 (G) and FOS (I) in the three groups.

Supplementary Files

This is a list of supplementary files associated with this preprint. Click to download.

- miR21transfected.zip
- SOX2transfected.zip
- differentiation.zip
- WB.pdf